Interactions between ferroelectric core-shell nanospheres and autocatalytic front reactions - Towards developing combined visual/RFID sensor labels utilizing pH-change based responses

Final project report

29 January, 2019

Contents

Concept and objectives

One of the challenges in indicator label development is the difficulty of translating color changes into electronic signals required for integrating the indicator units into data collection networks. Attaching the indicator to an optical fiber end and using UV-Vis spectroscopy for data acquisition is possible but increases size and cost and makes it difficult to integrate the unit into printed electronics. However, if the chemical front induced color change was coupled to a change in the dielectric properties of the reaction mixture, then it should be possible to detect the front propagation electronically. Unfortunately, the chemical front induced dielectric changes in a homogeneous aqueous system are very small as the high dielectric constant of the aqueous matrix masks the tiny differences in the relative permittivity of protonated and deprotonated species.

We addressed this challenge by creating the theoretical and experimental framework for a pH-response based indicator label which offers simultaneous visual feedback and passive RFID (Radio Field Identification) readout possibility by running an autocatalytic chemical front reaction in a nanoporous matrix constructed of ferroelectric core- shell nanospheres. We planned focus on the physical chemistry of the system. A proof-of-concept type model unit was planned, but making a prototype RFID tag was considered to be out of the scope of this fundamental research project.

Core results related to the main research topic

Preliminary experiments were carried out where the effect of transport processes - diffusion and advection -was studied separately in an autocatalytic crystallization reaction. Conditions of constant concentration gradients arising from the flow of reactants with appropriate density difference between the reactants were used to investigate the developed macrostructure and the corresponding microstructure. We have shown that the variation of the external flow rate is an elegant tool to control not only the crystal size and morphology but also the chemical composition. (papers: cpl, CrystEngComm 1 and 2)

Silica, amino-functionalized inorganic silica and zirconia nanoshells have been selected as HINS matrices to couple with an appropriate autocatalytic reaction. The chlorite oxidation of tetrathionate gives a simple, reproducible system where the hydrogen ion acts as the autocatalyst. The pH of the solution is set to basic (9 < pH < 11) to eliminate self-initiation. As a first step the characteristics of the HINS, like size distribution was determined. The typical diameter of the HINS utilized in our work was in the range of 500-600 nm. The hydrogen ion binding capability of the amino-functionalized HINS described by its base dissociation constant with a value of $(1.2 +- 0.1)*10^{-4}$ suggesting a stronger, and hence a more efficient, hydrogen ion removal than that of ammonia in water.

Two types of experiments were then performed. In one, the HINS were homogeneously distributed in an agarose gel loaded with the CT reactants. In the second, reactant loaded HINS were close packed and placed to connect two agarose gels containing the CT reactants. In the first setup, reaction–diffusion fronts with constant propagation velocity evolve when the reaction is run in thin planar slices of nanoshell-containing agarose gel to exclude all convection related effects. (see pccp paper by Lantos et al) The corresponding figure and caption below are copied from the PCCP paper for reference here.
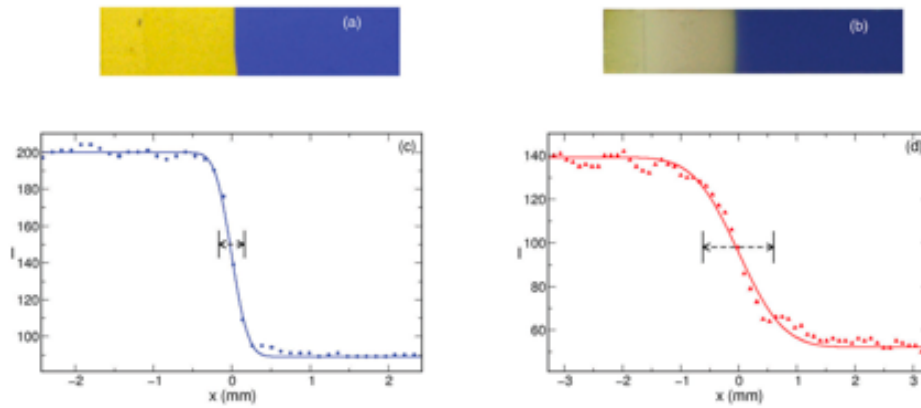
Fig. 2 Front images in the absence of nanoparticles at t = 7 min (a) and with 15 mg nanoparticle content at t = 230 min (b) with their front profiles (c and d) in gels of V = 8 cm³. The fitted cumulative normal distribution function is shown by solid lines and the appropriate front width is indicated with arrows. The length of the gel strips is 6.5 cm (a) and 5.8 cm (b).

By controlling the exact amount of amino-functionalized HINS in the gel matrix, it is possible to finely tune the propagation velocity of the chemical front in the 0.1-10 cm/h range. The effect of the binding on the front width has also been investigated. A cumulative normal distribution function is fitted to the sigmoid shape of the stable front profile, and the standard deviation associated with it is taken as the reaction front width. In the absence of the nanospheres, the front width is 200 micrometer which does not increase significantly until 40% of the hydrogen is bound by the HINS. The significant number of nanospheres makes the removal of hydrogen more efficient resulting in lower reaction rate and substantial widening of the reaction front. The larger front width also indicates the increasing contribution of diffusion to the evolving structure. Finally the macrostructure is investigated by carrying out the experiments in gel slices varying in their widths. Diffusion-driven instability does not develop as HINS is not immobilized in the gel, and the movement of the nanoparticles is freely possible. The corresponding figure and caption below are copied from the PCCP paper for reference here.
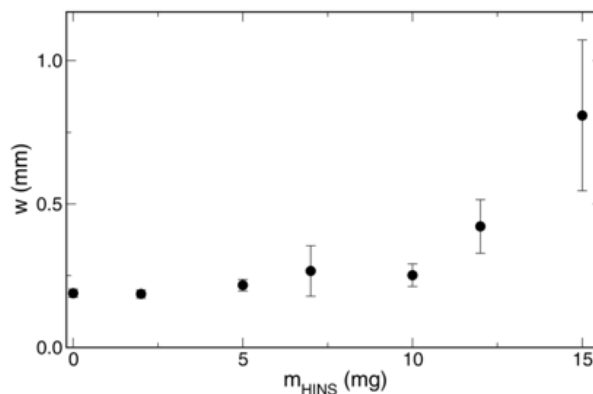

Fig. 5 Front width as a function of the nanosphere amount in gels of V = 8 cm³ in volume.

5

In the second configuration (see RSC Advances paper), we have investigated a system arising from the unidirectional coupling of HINS filled with the CT reactants. The corresponding figure and caption below are copied from the RSC Advances paper for reference here.
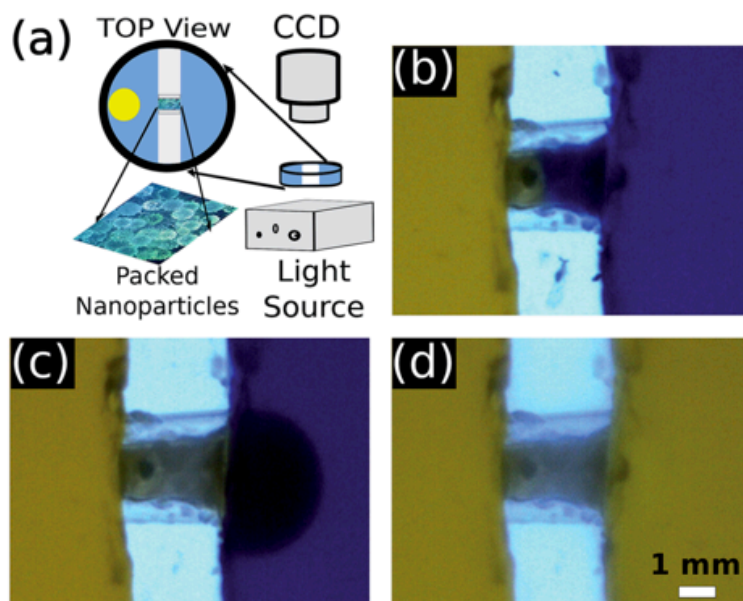

Fig. 2 Experimental setup (a). Snapshots 100 min (b), 390 min (c), and 395 min (d) after the front initiation. The dark blue areas correspond to reactants and the bright yellow areas to products, while the white areas represent the empty spaces separating the two gel pieces. The wave propagates from left to right. Field of view: 9.60 mm × 7.16 mm.

The suspension of HINS and the reactants is stirred to achieve uniform soaking of the nanoparticles. The suspension is then filtered and the filtrate is stored at room temperature before use. Two separate gel pieces are connected with a bridge formed by the close packing of the reactant loaded hollow and templated nanospheres employed as nanoreactors. A reaction-diffusion front is initiated in the agarose hydrogel which propagates through the gel with constant speed due to the coupling between reaction and diffusion. Then the front enters the bridge, propagates through it and upon exiting generates a new curved front. The time lapse images reveal that the front slows down significantly when it travels through the nanoshells. The slowing down inside the bridge arises because the HINS nanoreactors are spatially coupled via confined contact points with high curvature, through which the chemical front must pass as it travels across the cluster. This is also corroborated with a separate set of experiments where templated inorganic nanospheres are used instead of the hollow ones. Under such conditions there is no reactant solution within the nanospheres, no front propagation is observed through the bridge revealing that wave activity inside the nanospheres

is necessary for self-sustained propagation; reactant solutions wetting the outer surface of the templated nanospheres alone cannot support reaction-diffusion fronts. On the macroscale, the ensemble can sustain a pure reaction-diffusion front with constant velocity suggesting that a simple device based on the transmission of a chemical signal may be designed to amplify the change in hydrogen ion concentration through the use of hollow inorganic nanospheres. The corresponding figure and caption below are copied from the RSC Advances paper for reference here.
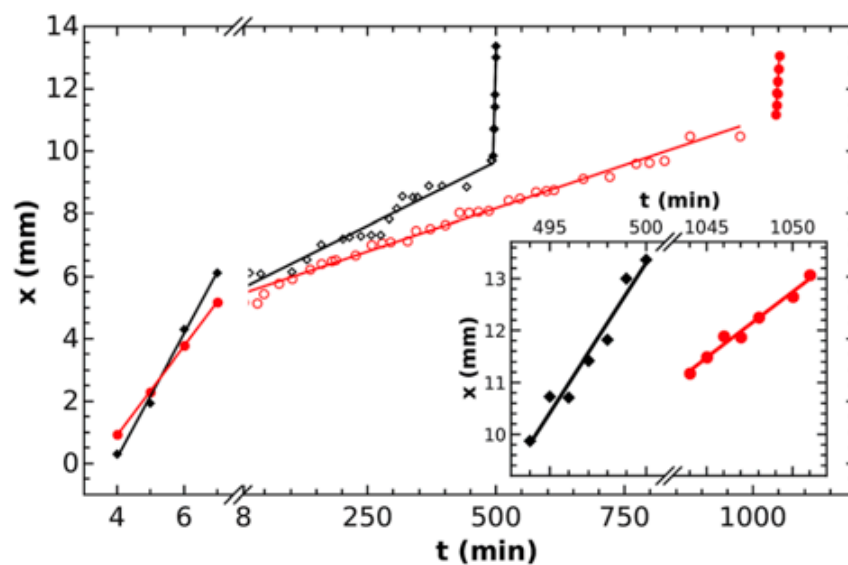

Fig. 4 Front position as a function of time for bridges of different length. The black diamonds and red circles correspond to cases with bridge length of 3.07 mm and 5.23 mm, respectively. The filled symbols depict the propagation in gel, the hollow ones that inside the bridge. The inset shows the wave propagation upon exiting the nanoparticle bridges.

7

General nanotechnology results with potential use for this project

Several interesting side topics have spawned from the present project, mostly in the fields of nanoparticle synthesis and heterogeneous catalysis based on the synthesized nanoparticles. These topics have been discussed in separate chapters of the annual project reports and published in peer-reviewed papers. Therefore, in the present report we cover only the results achieved in 2019, the final project year.

The work aimed at controlling the morphological properties (in particular, the diameter) of hollow inorganic nanospheres has contributed to our ongoing research on size-controlled Pt nanoparticles. A very interesting result in this field was that the size of Pt nanoparticles affects the hydrogen sensing behavior or Pt/WO_3 systems. The figure below is copied from the paper Mohl et al., JNN 2019, to illustrate this effect.
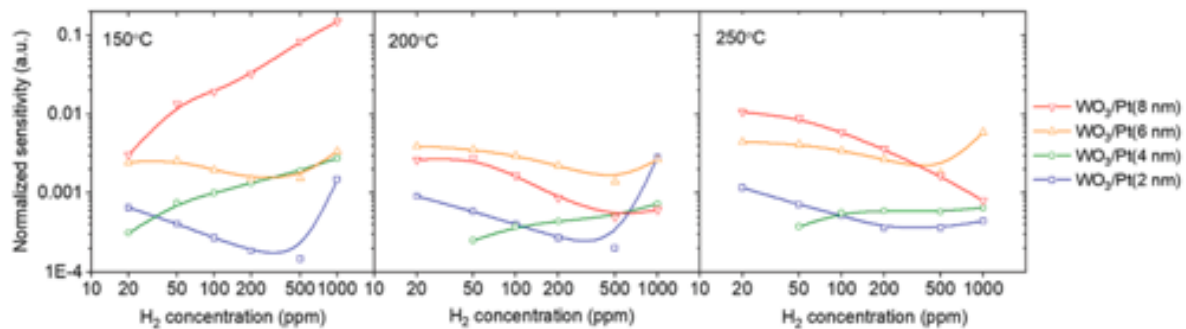

Figure 5. Sensor sensitivity normalized with Pt nanoparticle dispersion and concentration in the WO_3/Pt nanocomposites measured at 150, 200 and 250 °C.
Note: The lines (B-spline) connecting the discrete data points are only to guide the eye.

Furthermore, size-engineered Pt nanoparticles have been found to boost the catalytic activity of H-ZSM-5 zeolite in CO_2 activation. This is well evidenced by comparing the performance of Pt-free and 0.5% Pt containing H-ZSM-5 samples in the figure pair below (copied from Sapi et al., Frontiers in materials 2019).
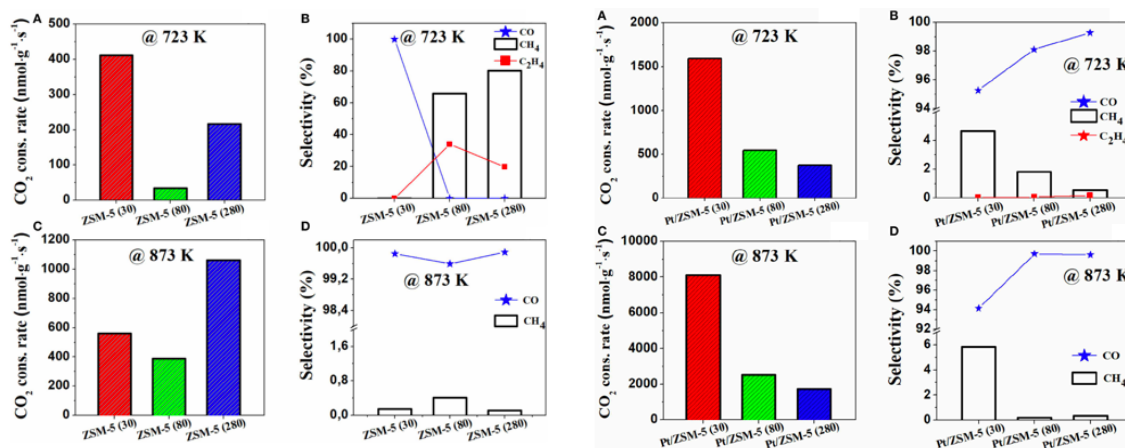
When investigating support effects on Pt nanoparticle decorated mesoporous oxide catalysts in CO2 hydrogenation, we have found Ni- and Co-based catalysts that produce methane with high selectivity as indicated by the figure below (copied from Sapi et al., J. CO_2 Util. 2019).
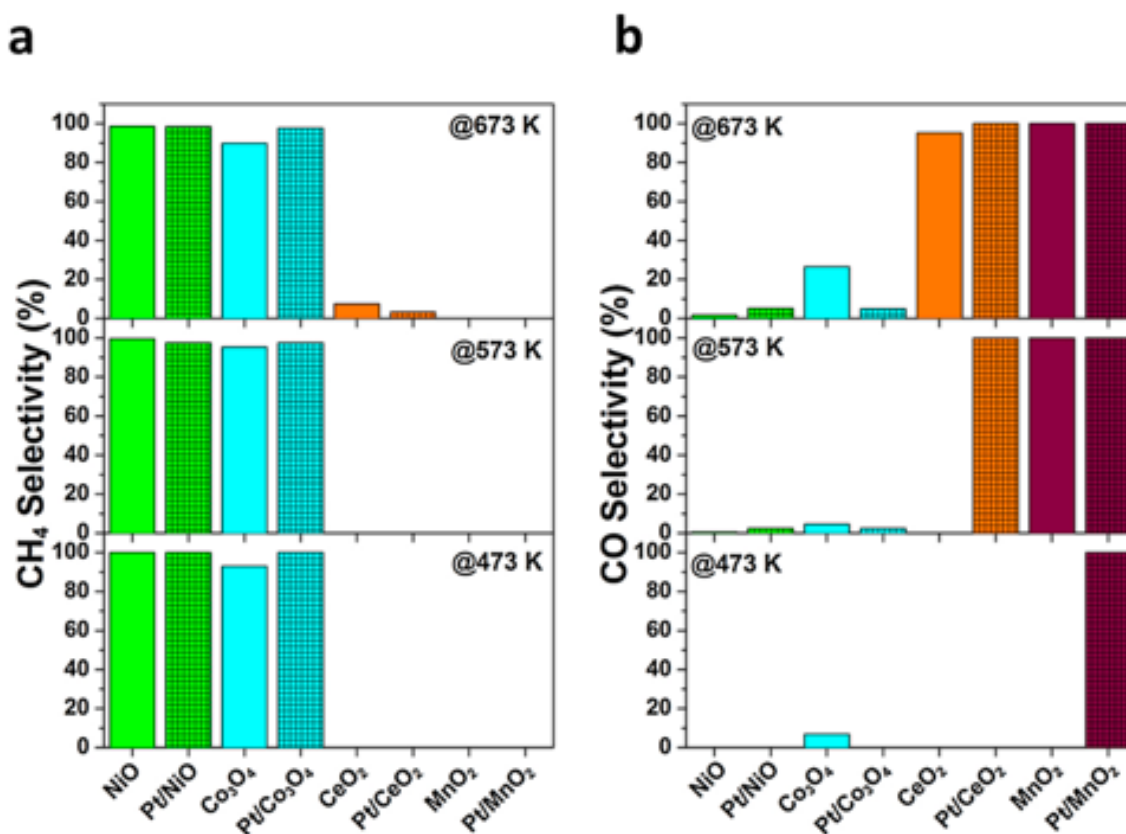

Fig. 8. Selectivity towards (a) CH_4 and (b) CO at 473 K, 573 K and 673 K.

A follow-up study focused on comparing Pt/Co_3O_4 and Pt/SBA-15 in CO_2 hydrogenation has revealed the temperature effects summarized in the figure below (copied from Sapi et al., JNN 2019).
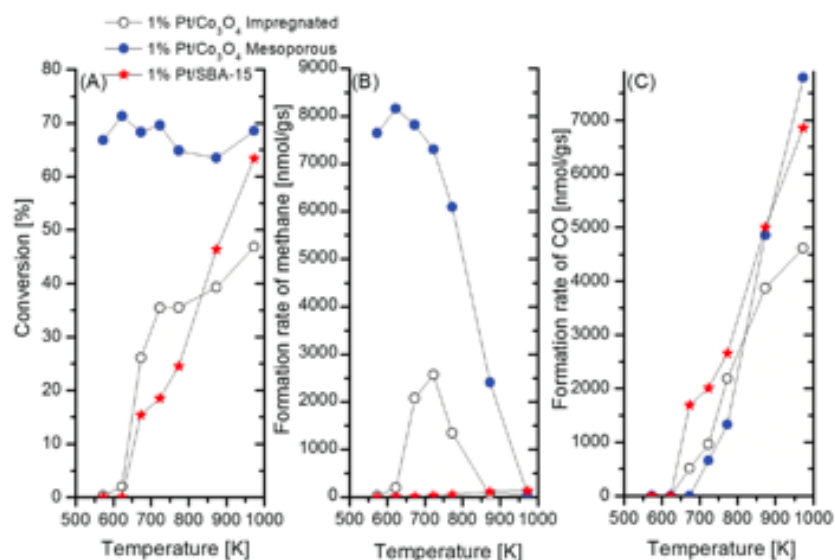
Figure 3. Effect of support in the hydrogenation of CO$_2$ on Pt anchored Merck Co$_3$O$_4$, mesoporous Co$_3$O$_4$ and SBA-15 catalysts. Conversion (A), formation rate of methane (B) and carbon-monoxide (C).

Palladium nanoparticles can be synthesized and used in similar ways as Pt nanoparticles. In 2019, we studied the restructuring of Pd nanoparticles supported over polydopamine as summarized below (figure copied from Gazdag et al., JNN 2019).
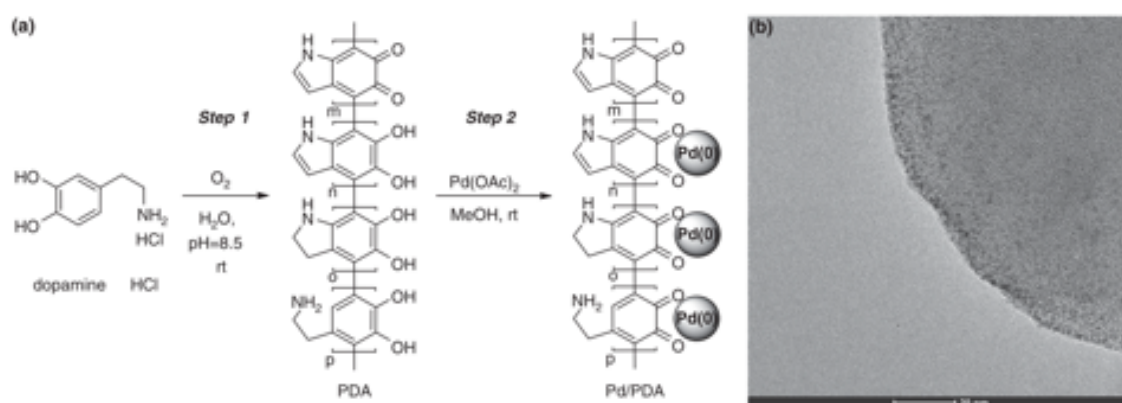

Figure 1. (a) Polymerization of dopamine hydrochloride to PDA (step 1) and Pd deposition onto the surface of PDA (step 2); (b) TEM image of Pd/PDA.

We have shown that both transfer hydrogenation and catalytic hydrogenation type reduction processes over polydopamine supported Pd catalyst are sensitive to the aggregation of Pd. In both cases decreased catalytic activity was associated with pronounced Pd particle aggregation. For transfer hydrogenation, the aggregation was found to be dependent on the nature of the H-source, for catalytic hydrogenation of a C=C double bond the H$_2$ atmosphere in combination with the substrate and different additives (CD, BA) played a crucial role. In the latter case the contribution of H$_2$ induced structural changes of PDA to particle aggregation cannot be ruled out.

10

Summary and self-assessment

The goal of this project was to study the interaction of hollow silica nanospheres and autocatalytic chemical front reactions. We achieved results in three main areas: (i) synthetic nanotechnology research with direct relevance to the project objectives, (ii) research directly related to autocatalytic front reactions, the main objectives of the project, and (iii) other results.

Our most important result is that we verified our main hypothesis. We were the first to demonstrate that close-packed hollow nanospheres containing a chemically active reactant medium inside can act as an assembly of nanoreactors with unidirectional coupling between them via autocatalytic front propagation. On the macroscale the ensemble can sustain a pure reaction-diffusion front with constant velocity suggesting that a simple device based on the transmission of a chemical signal may be designed to amplify the change in hydrogen ion concentration through the use of hollow inorganic nanospheres.

The least successful part of the project was the attempt to read out the progress of the autocatalytic front in the nanoreactors using RFID technology. Even though this experimental setup has been built and tested, we did not succeed in establishing reliable coupling between the front movement and the de-tuning of the passive RFID tag.

We published 50 peer-reviewed papers acknowledging this project during its 5-year lifetime. 49 out of these 50 were published in journals with an impact factor.

As for the specific objectives of the project, the following analysis can be given:

1. To develop the synthesis of submicron sized hollow inorganic nanospheres featuring a ferroelectric shell.

ACHIEVED PARTIALLY. We have established a very reliable synthesis route to yield hollow inorganic nanospheres (HINS) and we also succeeded in synthesizing spherical ferroelectric particles. However, it was not possible to prepare the latter ones in a hollow, shell-like morphology. Therefore, we decided to focus on HINS systems with silica walls.

2. What are the individual adsorption characteristics of the components of the appropriate chemical reaction on the chosen ferroelectric shell nanoparticles?

ACHIEVED: We have surveyed the filling characteristics of the HINS particles in detail and used this knowledge when planning the chemical front reactions.

3. What is the smallest H+ concentration change that results in a measurable variation of the dielectric response of a ferroelectric shell nanoparticle layer in an aqueous matrix?

ACHIEVED PARTIALLY: We have surveyed the H+ concentration effects on the system in detail. However, since the HINS did not have a ferroelectric shell, we had to drop the idea of inducing a measurable dielectric response variation.

4. Which polarization and/or charge carrier mobilization processes are responsible for this variation?

IRRELEVANT: due to the lack of a measurable dielectric response variation, this question became irrelevant.

5. What are the spatiotemporal evolution characteristics of pH-driven autocatalytic front reactions running in an immobilized aqueous matrix containing ferroelectric nanospheres?

ACHIEVED: the spatiotemporal front evolution characteristics were determined in detail and published.

6. Can the front propagation be influenced by an external electric field in this high-k dielectric environment? If yes, what are the details of the interaction mechanism?

ACHIEVED PARTIALLY: Our measurements have clearly indicated that an external electric field does not have a measurable effect on the front propagation. However, this the environment itself can not be considered a "high-k dielectric environment", we consider this objective to have been partially achieved only.

7. Can the front propagation be influenced by internal perturbations linked to the nanospheres? In particular, what is the effect of pH or reaction enthalphy induced localized HINS opening and subsequent release of the previously contained filler liquid (e.g. reactant, acid, base etc.)?

ACHIEVED: the response of the front to the internal characteristics of the HINS nanoreactors has been determined in detail and published.

8. To build a proof-of-concept type desktop model of the planned autocatalytic indicator label using a commercial flexible and transperent, printed RFID circuit as a basis.

ACHIEVED: the proof-of-concept type desktop model was built and tested using a commercial flexible RFID circuit.

All in all, we are proud of our achievements in this project. We opened a new research sub-field by boldly combining hollow spherical nanoreactors with autocatalytic front reactors for the first time, and we achieved several very interesting side results in the field of nanoparticle synthesis and nanoparticle based heterogeneous catalysis and sensors.